

**Activating Many-Body Localization in Solids by Driving with Light**Zala Lenarčič,<sup>1,2,\*</sup> Ehud Altman,<sup>2</sup> and Achim Rosch<sup>1</sup><sup>1</sup>*Institute for Theoretical Physics, University of Cologne, D-50937 Cologne, Germany*<sup>2</sup>*Department of Physics, University of California, Berkeley, California 94720, USA*

(Received 9 July 2018; published 28 December 2018)

Because of the presence of phonons, many-body localization (MBL) does not occur in disordered solids, even if disorder is strong. Local conservation laws characterizing an underlying MBL phase decay due to the coupling to phonons. We show that this decay can be compensated when the system is driven out of equilibrium. The resulting variations of the local temperature provide characteristic fingerprints of an underlying MBL phase. We consider a one-dimensional disordered spin chain, which is weakly coupled to a phonon bath and weakly irradiated by white light. The irradiation has weak effects in the ergodic phase. However, if the system is in the MBL phase, irradiation induces strong temperature variations despite the coupling to phonons. Temperature variations can be used similar to an order parameter to detect MBL phases, the phase transition, and a MBL correlation length.

DOI: [10.1103/PhysRevLett.121.267603](https://doi.org/10.1103/PhysRevLett.121.267603)

A quantum many-body system subjected to strong disorder can be many-body localized and thus fail to thermalize when evolving under its own dynamics [1,2]. This phenomenon has attracted a lot of interest as an example of a novel dynamical state of matter. In the case of a fully many-body localization (MBL) state, where all the many-body eigenstates of the Hamiltonian are localized, the system is characterized by an extensive set of local integrals of motion [3–10].

The local conservation laws persist without fine-tuning, which makes MBL more robust than conventional integrability. Like integrable models, however, many-body localization cannot survive even the weakest static coupling of the system to an external bath of delocalized excitations [11–24]. Any such coupling would lead to thermalization; therefore all direct experimental demonstrations of MBL so far have been achieved with ultracold atomic systems [25–27] as well as trapped ions [28], which can be extremely well isolated from the environment. In solids, by contrast, the electronic degrees of freedom are inevitably coupled to phonons and the ensuing thermal state shows no sign of the local integrals of motion.

In this Letter, we argue that the local integrals of motion of an electronic system can be “reactivated” by driving the system to a nonequilibrium steady state. In essence, the driving counters the relaxation with the phonon bath, giving rise to a new steady state in which the value of the local integrals of motion is set by a local balance between the phonons and the drive. In the limit of weak drive and weak coupling to phonons, this scheme allows us to make a sharp distinction between the steady states obtained with the dominant Hamiltonian in the MBL phase compared to an ergodic one, as demonstrated in Fig. 1.

In previous work, two of us developed a formalism for computing the steady-state density matrix of integrable systems subject to weak driving and coupling to baths [29–31], which is also applicable here. In the limit of weak driving steady-state expectation values can be approximately computed using a generalized Gibbs ensemble adjusted to expectation values of the integrals of motion, determined by rate equations. Figure 1 shows how this scheme plays out in the MBL phase compared to a conventional thermalizing phase. In the fully MBL system, there is always a set of integrals of motion related to the local energy density. Hence driving the system gives rise to widely varying local temperatures. In an ergodic system, on the other hand, only the global energy is conserved; hence when it is weakly driven the system equilibrates to a thermal state characterized by a single temperature.

In a similar setup with a disordered system weakly coupled to a bath and a monochromatic drive, Refs. [32,33] studied optimization of nuclear polarization. Nuclear polarization is optimized when the underlying system is close to the localization transition. In agreement with our results, they concluded that an equilibrium description in terms of spin temperature can be applied only in the ergodic phase. Persistent signatures of MBL have been observed also in system with Markovian dissipation where non-Hermitian Lindblad operators simultaneously drive and couple the system to baths [34]. Also, Ref. [35] has previously proposed a different approach to detect indirect signatures of many-body localization in electron systems. The emphasis of that work is on signatures of a finite temperature localization transition that persist despite the broadening of the transition due to coupling to phonons. Recently, possible indications of the proximity to such a transition were seen in a disordered InO film [36]. These

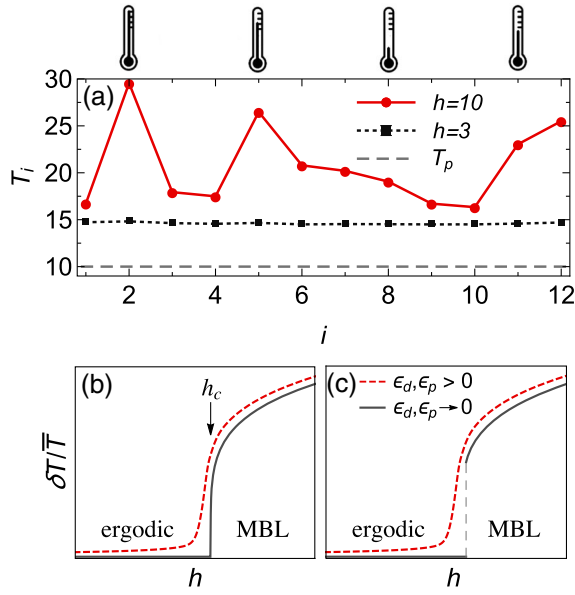


FIG. 1. (a) Profile of local temperatures in system coupled to a phonon bath at temperature  $T_p$  and driven weakly by white light. The temperature variations are large in the MBL phase (red circles), while they are vanishing in the ergodic phase (black squares). (b), (c) Fluctuations of the temperature can be used as an effective order parameter to detect a MBL transition. In the limit of vanishing coupling to the phonons and the drive,  $\epsilon_d, \epsilon_p \rightarrow 0$ , while  $\epsilon_d/\epsilon_p \rightarrow \text{const}$ , temperature fluctuation only arises in the MBL phase. Both a smooth transition (b) or a jump at the critical point (c) are consistent with our results obtained on small systems. Finite coupling,  $\epsilon_d, \epsilon_p > 0$ , is expected to smoothen the transition into a crossover.

effects are, however, indirect and may not be unique for MBL. The effects we discuss in this Letter, by contrast, provide a direct unambiguous signature of MBL.

Our goal is to describe a strongly disordered, interacting electron system in a solid weakly coupled to phonons and irradiated by light,  $H = H_f + H_p^0 + H_{fp} + H_d$ . To simplify the numerical analysis, we consider a one-dimensional model of spinless fermions with periodic boundary conditions at half-filling

$$H_f = \tilde{t} \sum_{i=1}^N (c_i^\dagger c_{i+1} + c_{i+1}^\dagger c_i) + V_i n_i + U n_i n_{i+1}, \quad (1)$$

which is related to the Heisenberg model of spins via Jordan-Wigner transformation. We use interaction strength  $U = 2$  corresponding to the isotropic point of the Heisenberg model. The lattice constant  $a$  is set to  $a = 1$  as well as  $\tilde{t} = 1$ . The random local potential  $V_i$  is drawn from a box distribution,  $V_i \in [-h, h]$ . This model and its variants [37–43] have been studied extensively and are known to show an (infinite temperature) MBL transition at a critical disorder strength of about  $h \approx 7$  (see, e.g., [38,39]).

The fermions interact with three dimensional acoustic phonons  $H_p^0 = \sum \omega_q a_q^\dagger a_q$  with dispersion  $\omega_q = v|\mathbf{q}|$ ,  $v = \tilde{t}$  which couple to the electrons through the hopping matrix element

$$H_{fp} = \epsilon_p \sum_{q_x} \int \frac{dq_x^2}{(2\pi)^2} (a_q + a_q^\dagger) \frac{iq_x}{\sqrt{2\omega_q}} H_{q_x},$$

$$H_{q_x} = \frac{1}{\sqrt{N}} \sum_j \tilde{t} e^{iq_x j} (c_{j+1}^\dagger c_j + c_j^\dagger c_{j+1}). \quad (2)$$

The dimensionless parameter  $\epsilon_p$  controls the strength of electron-phonon interaction. Because of periodic boundary conditions in  $x$ , the (dimensionless) momenta take quantized values  $q_x = (2\pi/N)n_x$ , while the perpendicular momenta are continuous. The three-dimensional phonons act as a thermal bath with a fixed temperature  $T_p$ .

At the same time, the system is driven out of equilibrium due to irradiation by white light arising, e.g., from a light bulb with a very high temperature  $T_d \gg \tilde{t}, h, T_p$ . The light couples to the current operator

$$H_d = \epsilon_d A(t) \sum_i \tilde{t} (c_{i+1}^\dagger c_i - c_i^\dagger c_{i+1}). \quad (3)$$

Here the dimensionless vector potential is given by  $\epsilon_d A(t)$ . We assume that  $A(t)$  is a delta-correlated classical field  $\langle A(t)A(t') \rangle = 2\pi\delta(t-t')$  and  $\epsilon_d$  parametrizes the amplitude of the electric fields. Note that a  $\delta$ -correlated vector potential corresponds to the electric field correlation  $\langle E_\omega E_{\omega'} \rangle \sim \delta(\omega + \omega')\omega^2$  expected for blackbody radiation for  $\omega \ll T_d$ .

We would like to obtain the steady-state of the driven interacting system in the limit of weak coupling to phonons and light. Formally, we first take the limit  $t \rightarrow \infty$  and afterwards the limit  $\epsilon_p, \epsilon_d \rightarrow 0$ . In this sequence of limits, the steady-state density matrix of the fermionic system is given by

$$\lim_{\epsilon_p, \epsilon_d \rightarrow 0} \lim_{t \rightarrow \infty} \rho(t) = \sum_n p_n |n\rangle \langle n|, \quad (4)$$

where  $|n\rangle$  are the exact many-particle eigenstates of  $H_f$ . The probabilities  $p_n$  depend sensitively on the couplings to phonons and to light, which determine the transition rates  $\Gamma_{mn} = \Gamma_{mn}^p + \Gamma_{mn}^d$  from state  $|n\rangle$  to state  $|m\rangle$ . The probabilities  $p_n$  are computed from the steady-state  $dp_n/dt = 0$  of the rate equation

$$\frac{d}{dt} p_n = \sum_m \Gamma_{nm} p_m - \Gamma_{mn} p_n. \quad (5)$$

The transition rates are derived using Fermi's golden; see Supplemental Material [44] for concrete expressions.

Properties of the obtained steady state are studied through the behavior of local temperatures at different sites. To define local temperatures out of equilibrium, we directly model a “thermometer” by infinitesimally coupling a bosonic bath with temperature  $T_j$  to the tunneling term  $c_j^\dagger c_{j+1} + c_{j+1}^\dagger c_j$ . The temperature  $T_j$  is determined from the condition that the energy current to the thermometer vanishes (see Supplemental Material for details [44]). Note that out of equilibrium the precise value of  $T_j$  depends on the type of thermometer one is using. However, the qualitative difference in behavior between the ergodic and MBL phases is not sensitive to such details. Experimentally, there are various methods to measure local temperatures, including the measurement of thermoreflectance [48], scanning thermal microscopy [49], and fluorescent microthermal imaging [50,51]. Finally, scanning light sources [52] for local Raman spectroscopy [53] with resolution of 10–20 nm can be used to obtain local temperatures by comparing Stokes and anti-Stokes lines of suitable transitions.

Figure 1(a) shows the local temperature profile calculated for one disorder configuration and a fixed ratio  $(\epsilon_d/\epsilon_p)^2 = 0.3$  in the limit  $\epsilon_d, \epsilon_p \rightarrow 0$ . Deep in the ergodic phase, the fluctuations of the local temperature are very small, whereas they become large in the MBL regime. We propose to use this as an experimental probe of MBL on solids.

We now turn to quantify the magnitude of local temperature fluctuation. For each disorder configuration  $n$  we determine the deviation of the local temperature  $T_{n,i}$  from the average temperature of the chain  $T_n \equiv (1/N) \sum_{i=1}^N T_{n,i}$ , that is,  $\delta T_{n,i} = T_{n,i} - T_n$ . The average fluctuation over all sites and disorder configurations is calculated from the variance of  $\delta T_{n,i}$ ,  $\delta T \equiv \sqrt{\langle \delta T_{n,i}^2 \rangle}$ . The average temperature is  $\bar{T} \equiv \langle T_{n,i} \rangle$ . In our numerical results, we average over  $M = 500$  random disorder configurations.

We expect that in the thermodynamic limit  $\delta T = 0$  in the ergodic phase, but is nonvanishing in the MBL phase [Fig. 1(b)]. Thus the temperature fluctuation serves similar to an order parameter of the MBL phase and is expected to grow with a universal exponent  $\alpha$  upon entering the phase

$$\lim_{N \rightarrow \infty, \epsilon_d, \epsilon_p \rightarrow 0} \frac{\delta T}{\bar{T}} \sim \begin{cases} 0 & \text{for } h < h_c \\ (h - h_c)^\alpha & \text{for } h > h_c. \end{cases} \quad (6)$$

Here the limit is taken with  $\epsilon_d/\epsilon_p = \text{const}$  and  $h_c$  is the critical disorder strength characterizing the MBL transition. Note that  $\delta T/\bar{T}$  could also jump, i.e., with  $\alpha = 0$  at the transition.

The vanishing of temperature variations for  $h < h_c$  follows from the fact that in the thermodynamic limit with  $\epsilon_d, \epsilon_p \rightarrow 0$  ergodic systems equilibrate to a thermal state characterized by a unique temperature (see Supplemental

Material for details [44]). For  $h > h_c$ , in contrast, an extensive set of local conservation laws prohibits equilibration, and we expect a highly nonthermal state arising from the solution of rate equations for which fluctuation dissipation relations are violated, leading to strongly fluctuating local temperatures.

Our numerical calculations are done on a finite size system with up to 12 sites. In this case, the sharp phase transition gives way to a smooth crossover [Fig. 2(a)]. We fix the phonon temperature to  $T_p = 10$ ; see Supplemental Material for a discussion of the dependence on  $T_p$  [44].

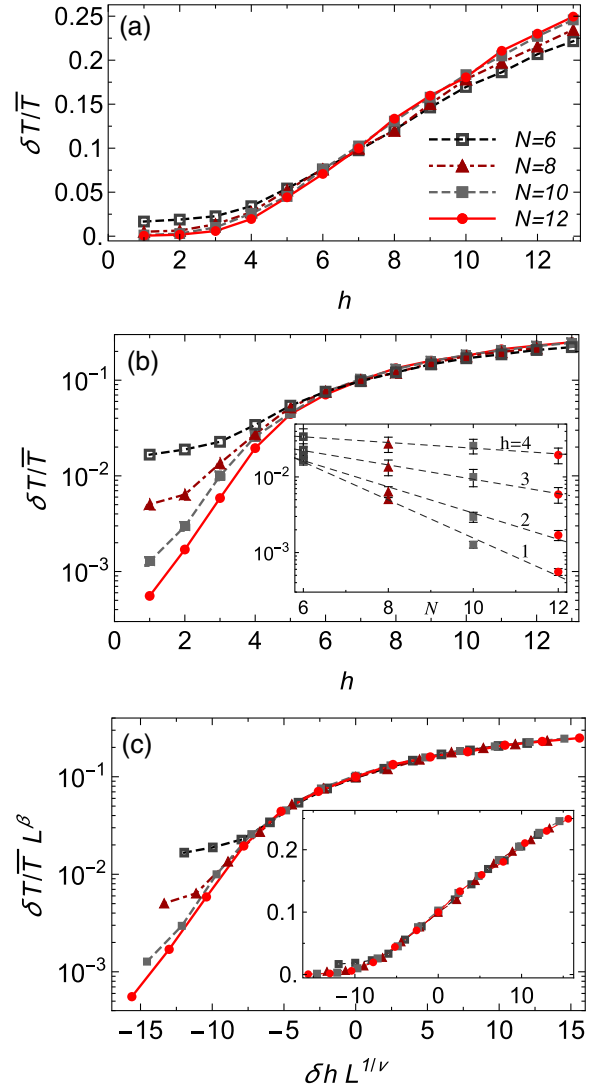


FIG. 2. (a) Average fluctuation of local temperatures  $\delta T$  normalized by the average temperature  $\bar{T}$  as function of disorder strength  $h$  for the system sizes  $N = 6, 8, 10, 12$ . (b) The logarithmic plot shows that  $\delta T/\bar{T}$  drops exponentially in system size in the ergodic phase, Eq. (7). The  $N$  dependence for small  $h$  is shown in the inset. (c) A data collapse is obtained by rescaling using  $h_c = 7, \nu = 2.6, \beta = 0$ . Inset: Same scaling plot on a linear scale. Parameters:  $T_p = 10, U = 2, (\epsilon_d/\epsilon_p)^2 = 0.3$ .

In the ergodic phase, we find that  $\delta T$  drops as a function of system size in a manner consistent with exponential dependence [Fig. 2(b)],

$$\frac{\delta T}{\bar{T}} \sim e^{-L/\xi_e(h)}. \quad (7)$$

The decay length  $\xi_e(h)$  grows rapidly on approaching the MBL transition; see Fig. 3; hence we associate it with the correlation length that diverges at the critical point as  $\xi_e \sim [1/(h_c - h)^\nu]$ .

It is instructive to apply a finite size scaling analysis. Figure 2(c) shows a scaling collapse of the data assuming a universal scaling function  $(\delta T/\bar{T}) = L^{-\beta} f(L^{1/\nu} \delta h)$ ,  $\delta h = h - h_c$ . This scaling function also implies that  $(\delta T/\bar{T}) \sim (h - h_c)^{\beta\nu}$  on crossing the transition. To obtain collapse, we assumed  $h_c = 7$  and fitted  $\nu \approx 2.6$ ,  $\beta \approx 0$ . Latter values are consistent also with the fit to  $\xi_e(h_c - h)$  (see inset of Fig. 3). However, we cannot precisely determine  $h_c$  from our data since reasonable data collapse can be obtained within a range of parameters, giving rise to crude estimates  $h_c \approx 6.5 \pm 1$  (consistent with exact diagonalization results, e.g., [39]),  $\nu = 2.5 \pm 0.5$ , and  $\beta = 0.08 \pm 0.08$ . It is interesting that we find a value of  $\nu$  consistent with the Chayes-Harris bound [54–56],  $\nu > 2/d$ , where  $d$  is the spatial dimension. This is in marked contrast with results of exact diagonalization studies, which obtain  $\nu \approx 1$ , e.g., [39]. Rather, the result is closer to the renormalization group approaches [57,58], which obtain  $\nu \approx 3.3$ .

On the MBL side, we expect that  $\delta T_j$  fluctuates on short scales associated with the localization length  $\xi_l$ . The correlation function  $C(\delta) = \langle (T_{n,i} - \bar{T})(T_{n,i+\delta} - \bar{T}) \rangle$  is plotted in Fig. 4. We determine  $\xi_l$  from the fit  $C(\delta) \sim e^{-\delta/\xi_l(h)} + e^{-(N-\delta)/\xi_l(h)}$ .

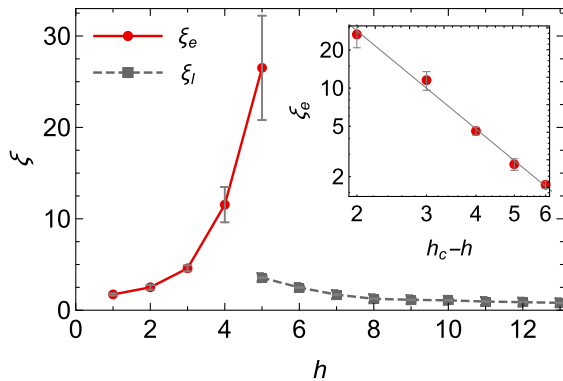


FIG. 3. Correlation length as function of the disorder strength  $h$ . For small  $h$  the correlation length is defined by Eq. (7), see Fig. 2. For large  $h$  it is calculated from the spatial correlations of  $\delta T$  discussed in Fig. 4. (Inset) The critical exponent  $\nu$  can be extracted from the fit  $\xi_e \sim [1/(h_c - h)^\nu]$ . We get  $\nu \approx 2.6$  assuming  $h_c = 7$  (see text).

$\xi_l(h)$  is shown in Fig. 3 together with  $\xi_e(h)$  obtained from Eq. (7).  $\xi_l(h)$  grows with decreasing disorder, but unlike  $\xi_e(h)$  on the ergodic side, it does not seem to diverge at the critical point. This behavior is consistent with other numerical results and renormalization group approaches [57,58], which also fail to extract a diverging localization length from the behavior of typical physical quantities. Indications of a diverging localization length manifest only when considering special quantities, whose average is sensitive to the appearance of rare thermalizing clusters that ultimately trigger the phase transition to the ergodic phase [57].

The analysis discussed above is rigorously valid in the limit  $\epsilon_p, \epsilon_d \rightarrow 0$ . At finite  $\epsilon_p$  and  $\epsilon_d$  nonzero fluctuations  $\delta T$  are expected also in the ergodic phase. Deep in the ergodic phase,  $\delta T$  can be calculated from a straightforward hydrodynamic approach describing the interplay of heat conduction and local heating and cooling by light and phonons, respectively (see Supplemental Material [44]). From this analytic approach, we obtain in  $d$  dimensions deep in the ergodic phase

$$\delta T \sim \frac{1}{\bar{\kappa}^{d/4}} \left( \frac{\epsilon_d}{\epsilon_p} \right)^2 \epsilon_p^{d/2}, \quad (8)$$

where  $\bar{\kappa}$  is the (average) heat conductivity. As expected, for  $\epsilon_p, \epsilon_d \rightarrow 0$  at fixed ratio  $\epsilon_d/\epsilon_p$ ,  $\delta T$  vanishes. Remarkably, the same hydrodynamic approach predicts that  $\delta T$  is of order 1 in the MBL phase (see Supplemental Material [44]).

As  $\delta T$  is finite in the ergodic phase for finite  $\epsilon_{p,d}$ , the sharp transition in  $\delta T$  expected for  $\epsilon_d, \epsilon_p \rightarrow 0$ , Eq. (6), will be broadened for finite  $\epsilon_d, \epsilon_p$  (see Fig. 1). In an actual solid-state experiment, one easily controls  $\epsilon_d$  by changing the radiation density but not the strength of phonon coupling. A lowering of temperature does, however, essentially have the same effect as a reduction of  $\epsilon_p$ , as the ability to cool the

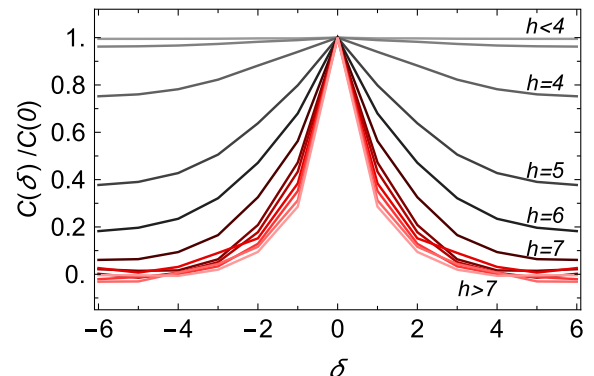


FIG. 4. Correlation function of the local temperature defined by  $C(\delta) = \langle (T_{n,i} - \bar{T})(T_{n,i+\delta} - \bar{T}) \rangle$ . In the MBL phase, temperature fluctuates on a rather short length scale associated with the localization length  $\xi_l$ . Parameters:  $N = 12$ ,  $T_p = 10$ ,  $U = 2$ ,  $(\epsilon_d/\epsilon_p)^2 = 0.3$ .



system strongly depends on  $T_p$  (see Supplemental Material [44]). By simultaneously lowering temperature and irradiation, it should be possible to approach systematically the limit  $\epsilon_d, \epsilon_p \rightarrow 0$ .

Finally, we discuss possible experimental realizations. Experiments with disordered indium oxide films have shown clear signatures of decoupling between the electron and phonon temperatures, which occurs due to driving the system with voltage together with the weakness of the electron-phonon interaction at low temperature [59]. Furthermore, precursors of a many-body localization transition at finite  $T$  have been reported in the same films [36]. Hence, we believe this system is a promising test bed for investigating many-body localization in the approach developed in this Letter. Furthermore, it is promising to search for signatures of many-body localization in weakly doped semiconductors, which have been studied intensively [60] in the context of the Anderson transition.

An important challenge is to identify suitable local probes that would allow us to measure the local electronic temperature. One promising approach is to use scanning light sources [52] for local Raman spectroscopy [53], which would be sensitive to the local temperature through the ratio of the Stokes and anti-Stokes peak amplitudes. Their resolution of 10–20 nm is comparable to the expected correlation length of temperature fluctuations. Note that such a fine resolution is actually unnecessary since even averaging over  $N_{\text{av}}$  uncorrelated regions would reduce the temperature fluctuations only by a factor  $\sqrt{N_{\text{av}}}$ .

Our analysis in this Letter mainly focused on the limit of weak coupling to the phonons and the drive, i.e.,  $\epsilon_p, \epsilon_d \rightarrow 0$  while keeping  $\epsilon_d/\epsilon_p$  constant. A complete understanding of the driven system at finite  $\epsilon_{p,d}$  requires further study. In particular, it would be interesting to include the coupling to drive and to phonons within an effective description of the Griffiths phase and the MBL critical point [57]. In addition, tensor network techniques can be used to solve for the steady-state density matrix of the appropriate Lindblad evolution. Such studies could shed light on how the onset of  $\delta T/\bar{T}$  broadens into a universal crossover with increasing  $\epsilon_p, \epsilon_d$  and thus assist the interpretation of experiments that are necessarily done at finite coupling.

We acknowledge useful discussions with O. Alberton, M. Knap, and F. Lange. Z. L. and A. R. were financially supported by the German Science Foundation under CRC 1238 (project C04) while E. A. acknowledges the ERC synergy grant UQUAM.

---

\*zala.lenaric@berkeley.edu

- [1] D. Basko, I. Aleiner, and B. Altshuler, *Ann. Phys. (Amsterdam)* **321**, 1126 (2006).  
 [2] I. V. Gornyi, A. D. Mirlin, and D. G. Polyakov, *Phys. Rev. Lett.* **95**, 206603 (2005).

- [3] R. Vosk and E. Altman, *Phys. Rev. Lett.* **110**, 067204 (2013).  
 [4] M. Serbyn, Z. Papić, and D. A. Abanin, *Phys. Rev. Lett.* **111**, 127201 (2013).  
 [5] D. A. Huse, R. Nandkishore, and V. Oganesyan, *Phys. Rev. B* **90**, 174202 (2014).  
 [6] V. Ros, M. Müller, and A. Scardicchio, *Nucl. Phys.* **B891**, 420 (2015).  
 [7] A. Chandran, I. H. Kim, G. Vidal, and D. A. Abanin, *Phys. Rev. B* **91**, 085425 (2015).  
 [8] T. E. O'Brien, D. A. Abanin, G. Vidal, and Z. Papić, *Phys. Rev. B* **94**, 144208 (2016).  
 [9] M. Mierzejewski, M. Kozarzewski, and P. Prelovšek, *Phys. Rev. B* **97**, 064204 (2018).  
 [10] M. Goihl, M. Gluza, C. Krumnow, and J. Eisert, *Phys. Rev. B* **97**, 134202 (2018).  
 [11] M. Žnidarič, *New J. Phys.* **12**, 043001 (2010).  
 [12] R. Nandkishore, S. Gopalakrishnan, and D. A. Huse, *Phys. Rev. B* **90**, 064203 (2014).  
 [13] S. Johri, R. Nandkishore, and R. N. Bhatt, *Phys. Rev. Lett.* **114**, 117401 (2015).  
 [14] M. H. Fischer, M. Maksymenko, and E. Altman, *Phys. Rev. Lett.* **116**, 160401 (2016).  
 [15] M. V. Medvedyeva, T. Prosen, and M. Žnidarič, *Phys. Rev. B* **93**, 094205 (2016).  
 [16] P. Bordia, H. P. Lüschen, S. S. Hodgman, M. Schreiber, I. Bloch, and U. Schneider, *Phys. Rev. Lett.* **116**, 140401 (2016).  
 [17] P. Prelovšek, *Phys. Rev. B* **94**, 144204 (2016).  
 [18] E. Levi, M. Heyl, I. Lesanovsky, and J. P. Garrahan, *Phys. Rev. Lett.* **116**, 237203 (2016).  
 [19] H. P. Lüschen, P. Bordia, S. S. Hodgman, M. Schreiber, S. Sarkar, A. J. Daley, M. H. Fischer, E. Altman, I. Bloch, and U. Schneider, *Phys. Rev. X* **7**, 011034 (2017).  
 [20] D. J. Luitz, F. Huveneers, and W. De Roeck, *Phys. Rev. Lett.* **119**, 150602 (2017).  
 [21] R. Nandkishore and S. Gopalakrishnan, *Ann. Phys. (Berlin)* **529**, 1600181 (2017).  
 [22] B. Everest, I. Lesanovsky, J. P. Garrahan, and E. Levi, *Phys. Rev. B* **95**, 024310 (2017).  
 [23] J. Marino and R. M. Nandkishore, *Phys. Rev. B* **97**, 054201 (2018).  
 [24] A. Rubio-Abadal, J. Choi, J. Zeiher, S. Hollerith, J. Rui, I. Bloch, and C. Gross, [arXiv:1805.00056](https://arxiv.org/abs/1805.00056).  
 [25] M. Schreiber, S. S. Hodgman, P. Bordia, H. P. Lüschen, M. H. Fischer, R. Vosk, E. Altman, U. Schneider, and I. Bloch, *Science* **349**, 842 (2015).  
 [26] H. P. Lüschen, P. Bordia, S. Scherg, F. Alet, E. Altman, U. Schneider, and I. Bloch, *Phys. Rev. Lett.* **119**, 260401 (2017).  
 [27] A. Lukin, M. Rispoli, R. Schittko, M. E. Tai, A. M. Kaufman, S. Choi, Soonwon, V. Khemani, J. Léonard, and M. Greiner, [arXiv:1805.09819](https://arxiv.org/abs/1805.09819).  
 [28] J. Smith, A. Lee, P. Richerme, B. Neyenhuis, P. W. Hess, P. Hauke, M. Heyl, D. A. Huse, and C. Monroe, *Nat. Phys.* **12**, 907 (2016).  
 [29] F. Lange, Z. Lenarčič, and A. Rosch, *Nat. Commun.* **8**, 15767 (2017).  
 [30] Z. Lenarčič, F. Lange, and A. Rosch, *Phys. Rev. B* **97**, 024302 (2018).

- [31] F. Lange, Z. Lenarčič, and A. Rosch, *Phys. Rev. B* **97**, 165138 (2018).
- [32] A. De Luca and A. Rosso, *Phys. Rev. Lett.* **115**, 080401 (2015).
- [33] A. De Luca, I. R. Arias, M. Müller, and A. Rosso, *Phys. Rev. B* **94**, 014203 (2016).
- [34] I. Vakulchyk, I. Yusipov, M. Ivanchenko, S. Flach, and S. Denisov, *Phys. Rev. B* **98**, 020202 (2018).
- [35] D. M. Basko, I. L. Aleiner, and B. L. Altshuler, *Phys. Rev. B* **76**, 052203 (2007).
- [36] M. Ovadía D. Kalok, I. Tamir, S. Mitra, B. Sacépé, and D. Shahar, *Sci. Rep.* **5**, 13503 (2015).
- [37] V. Oganesyan and D. A. Huse, *Phys. Rev. B* **75**, 155111 (2007).
- [38] A. Pal and D. A. Huse, *Phys. Rev. B* **82**, 174411 (2010).
- [39] D. J. Luitz, N. Laflorencie, and F. Alet, *Phys. Rev. B* **91**, 081103 (2015).
- [40] S. D. Geraedts, N. Regnault, and R. M. Nandkishore, *New J. Phys.* **19**, 113021 (2017).
- [41] Y. Bar Lev, G. Cohen, and D. R. Reichman, *Phys. Rev. Lett.* **114**, 100601 (2015).
- [42] S. Bera, H. Schomerus, F. Heidrich-Meisner, and J. H. Bardarson, *Phys. Rev. Lett.* **115**, 046603 (2015).
- [43] M. Žnidarič, T. Prosen, and P. Prelovšek, *Phys. Rev. B* **77**, 064426 (2008).
- [44] See Supplemental Material at <http://link.aps.org/supplemental/10.1103/PhysRevLett.121.267603> for a comparison of local temperatures to the temperature obtained from a thermal ansatz and a discussion, which includes Refs. [45–47].
- [45] J. M. Deutsch, *Phys. Rev. A* **43**, 2046 (1991).
- [46] M. Srednicki, *Phys. Rev. E* **50**, 888 (1994).
- [47] M. Rigol, V. Dunjko, and M. Olshanii, *Nature (London)* **452**, 854 (2008).
- [48] D. G. Cahill *et al.*, *Appl. Phys. Rev.* **1**, 011305 (2014).
- [49] L. Cui *et al.*, *Nat. Commun.* **8**, 14479 (2017).
- [50] M. Otter *et al.*, *Int. J. Heat Mass Transfer* **55**, 2531 (2012).
- [51] D. Barton and P. Tangyunyong, *Microelectron. Eng.* **31**, 271 (1996).
- [52] A. Sternbach *et al.*, arXiv:1706.08478.
- [53] M. S. Anderson, *Appl. Phys. Lett.* **76**, 3130 (2000).
- [54] A. B. Harris, *J. Phys. C* **7**, 3082 (1974).
- [55] J. T. Chayes, L. Chayes, D. S. Fisher, and T. Spencer, *Phys. Rev. Lett.* **57**, 2999 (1986).
- [56] A. Chandran, C. R. Laumann, and V. Oganesyan, arXiv:1509.04285.
- [57] R. Vosk, D. A. Huse, and E. Altman, *Phys. Rev. X* **5**, 031032 (2015).
- [58] A. C. Potter, R. Vasseur, and S. A. Parameswaran, *Phys. Rev. X* **5**, 031033 (2015).
- [59] M. Ovadía, B. Sacépé, and D. Shahar, *Phys. Rev. Lett.* **102**, 176802 (2009).
- [60] H. Stupp, M. Hornung, M. Lakner, O. Madel, and H. v. Löhneysen, *Phys. Rev. Lett.* **71**, 2634 (1993).